Am J Cancer Res 2022;12(7):3111-3127
www.ajcr.us /ISSN:2156-6976/ajcr0143469

Original Article

LncRNA MEG3 inhibits retinoblastoma invasion and metastasis by inducing β-catenin degradation

Yali Gao[1*], Xiaona Chen[1*], Jun Zhang[2]

[1]Department of Ophthalmology, Shenzhen People's Hospital (The Second Clinical Medical College, Jinan University), Shenzhen 518020, Guangdong, China; [2]Department of Reproductive Medicine, Obstetrics and Gynecology, Shenzhen People's Hospital (The Second Clinical Medical College, Jinan University), Shenzhen 518020, Guangdong, China. [*]Equal contributors.

Received April 11, 2022; Accepted June 8, 2022; Epub July 15, 2022; Published July 30, 2022

Abstract: In our previous study, we found that low expression of LncRNA-MEG3 was closely associated with the invasion and metastasis of retinoblastomas. The molecular mechanism by which MEG3 inactivation induces the invasion and metastasis of retinoblastoma cell lines remains unclear. We used the GEO database to analyze the expression of MEG3 in retinoblastoma tissues and MEG3-related pathways. The scratch, transwell migration, mouse tumor metastasis, and mouse fluorescence live imaging assays were performed to detect migration and invasion of retinoblastoma cell lines. The RNA pull down, electrophoretic mobility shift, RIP, co-immunoprecipitation, and ubiquitination assays were performed to analyze the molecular mechanisms. The GEO database showed that the expression of MEG3 was low in retinoblastoma tissues and was closely associated with the invasion of retinoblastoma cells and activity of the Wnt pathway. Both *in vivo* and *in vitro* experiments confirmed that MEG3 inhibited the migration and invasion of retinoblastoma cells. Cell experiments confirmed that MEG3 could promote the binding of β-catenin and GSK-3β and induce phosphorylation, ubiquitination and degradation of β-catenin indirectly. In conclusion, MEG3 can promote the degradation of β-catenin via GSK-3β, which in turn inactivates the Wnt pathway and ultimately inhibits the invasion and metastasis of retinoblastoma cells.

Keywords: Retinoblastoma, LncRNA, MEG3, β-catenin, GSK-3β

Introduction

Retinoblastomas are the most common primary malignant tumor of the eye in infants and children, with a worldwide incidence of approximately 1:15,000-1:20,000 and approximately 9,000 new cases per year, mostly in Asia and Africa. There are approximately 1,000 new cases per year in China [1-3]. The survival rate of children with retinoblastoma in China remains low, which is mainly because most children with retinoblastoma in China are already in stage (II-IV) upon diagnosis, where the incidence of tumor invasion and metastasis is high and the treatment outcome is poor [4, 5]. Therefore, it is of great significance to elucidate the molecular mechanism of the invasion and metastasis of retinoblastomas to provide new diagnostic and treatment plans for patients and improve the survival rate and quality of life of patients.

Recent studies have found aberrant expression of long non-coding RNAs (lncRNAs) in various tumors, such as cervical cancer, colorectal cancer, and gastric cancer [6-10]. This can regulate the invasion of tumors through multiple signaling pathways. In our previous study, we examined the expression of MEG3 in 63 retinoblastoma and paraneoplastic normal retinal tissues and found that the level of MEG3 was remarkable lower in retinoblastoma tissues than in the paraneoplastic tissues. The low expression of MEG3 was significantly associated with lymph node and distant metastasis. The survival analysis found that the prognosis of Rb patients with low MEG3 expression was poor, thus proving that MEG3 has important clinical significance. Additionally, cellular experiments confirmed that MEG3 could inhibit proliferation and promote apoptosis of retinoblastoma cells. More important, MEG3 could inhibit Wnt path-

way via reducing the expression of β-catenin in retinoblastoma cell lines [11, 12]. However, the exact molecular mechanism remains unclear.

In this study, we first verified the low expression of MEG3 in retinoblastoma tissues through the Gene Expression Omnibus (GEO) database and analyzed the signaling pathways associated with MEG3. Subsequently, the effects of MEG3 on the migration and invasion of retinoblastoma cells were examined using *in vitro* and *in vivo* experiments. Finally, through the RNA pull down, electrophoretic mobility shift, RNA immunoprecipitation chip (RIP), co-immunoprecipitation, CHX assays and ubiquitination assays, it was confirmed that MEG3 may promote the binding of β-catenin and Glycogen synthase kinase-3β (GSK-3β), thereby inducing the phosphorylation, ubiquitination, degradation of β-catenin indirectly, leading to the inactivation of the Wnt pathway and ultimately inhibiting the invasion and metastasis of retinoblastoma cells. In this study, we attempted to determine new markers and biotherapeutic targets for the diagnosis and treatment of metastatic retinoblastomas by an in-depth exploration of the mechanism of metastatic retinoblastomas.

Materials and methods

Collection and preservation of specimens

The 63 retinoblastoma tissue specimens used in this study were the same as in our previous study [11]. The experimental procedures used in this study were approved by the Ethics Committee of Shenzhen People's Hospital (approval no. LL-KT-2019104). All patients in the experimental group provided their informed consent by signing the informed consent form.

Cell lines and culture conditions

The retinoblastoma cell lines Y79 and Weri-Rb1 were obtained from the ATCC cell bank (American Type Culture Collection, USA). Both cell lines were cultured in a medium containing RPMI 1640 and 10% fetal bovine serum at 37°C in an incubator with 5% CO_2. The medium was changed every 2-3 d.

Transient transfection of oligonucleotide

PcDNA-NC, PcDNA-MEG3, si-MEG3, and si NC were designed and synthesized by GenePharma (Shanghai, China), and the siRNA sequences used are shown in Table S1. The transfections were performed according to the manufacturer's instructions for Lipofectamine 2000 (Invitrogen, USA) and Opti MEM medium (Invitrogen, USA). Oligonucleotides were mixed thoroughly with the transfection reagents and placed at room temperature for 5 min before being added to the cell culture plates. Then, they were placed in an incubator for transfection. The solution was replaced with a general medium after 12 h to continue the cell culture.

Construction of stably transfected cell lines using lentiviral vectors

The lentiviral vector over-expressing MEG3 and its control lentiviral vector and the lentiviral vector expressing shRNA MEG3 and its control lentiviral vector were purchased from Shanghai GenePharma, Ltd. The groups were named as MEG3, Vector NC, shRNA MEG3, and shRNA NC. The shRNA sequences are shown in Table S1. Cell transfection was performed as per the lentiviral protocol, where healthy Y79 and Weri-Rb1 cells were inoculated in a 12-well plate at 0.5×10^5 cells/well and allowed to grow until 40% to 50% confluence is reached. Then, they were cultivated by adding 1×10^7 U/mL of lentivirus and a complete medium containing 5 μg/mL of polybrene. The cell culture was replaced with fresh medium after 24 h, and the virus infection was observed under a fluorescence microscope after 72 h. The culture medium containing 2 μg/mL of puromycin was used, and the medium was changed every 2 d. Stable cell lines were obtained after 2 weeks.

RNA extraction and quantitative reverse transcription-polymerase chain reaction (qRT-PCR)

Total RNA was extracted from the retinoblastoma cell line using the TRIzol reagent (TaKaRa, Japan) as per the manufacturer's instructions. The RNA samples were treated with DNase after the Trizol and a no sample negative control was done for general contamination. cDNA was reverse-transcribed from the extracted RNA using the M-MLV Reverse Transcription Kit (Thermo Fisher Scientific). The PCR reaction system was prepared as per the instructions of the SYBR Premix Ex Taq GC Kit (Thermo Fisher Scientific) and a 7900HT fast real-time PCR detection system (Thermo Fisher Scientific) was used for the qRT-PCR analysis. Primers were

synthesized by Invitrogen, and the sequences are listed in Table S2. Results were normalized to the expression of β-actin, and the expression of target genes relative to β-actin was calculated and normalized using the $2^{-\Delta\Delta Ct}$ method.

Western blotting assay

Proteins were extracted from cells in the logarithmic growth phase using RIPA (Thermo Scientific, USA) and were quantified using a BCA protein quantification kit (Tiangen, Beijing, China). To each well of the 10% SDS-PAGE gel, 50 μg of protein was added. After electrophoresis, the proteins were transferred to poly vinylidene fluoride (PVDF) membranes and blocked in 5% skimmed milk at room temperature for 2 h. The membranes were washed three times with TBST, and then primary antibodies against β-catenin, GSK-3β, and β-actin (CST, USA, 1:1000) were added and incubated overnight at 4°C. The membranes were then washed three times with TBST and the secondary antibody of HRP-labeled goat anti-rabbit IgG (Santa Cruz, USA, 1:2000) was added. The membranes were incubated for 2 h at room temperature, developed with the ECL solution (Thermo Scientific, USA), and imaged using a GBOX gel imaging system and the accompanying software (Genesys, France).

Scratch test

Y79 and Weri-Rb1 cells were inoculated into 6-well plates at 5×10^4 cells per well, and three replicate wells were used for each group of cells. Cells were incubated at 37°C with 5% CO_2 for 24 h. After incubation, a cell-free trace of approximately 1 mm in width was drawn at the bottom of the 6-well plates with an autoclaved 10 μL pipette tip. PBS was used to rinse the plate three times to remove the cells that were scratched off thoroughly. Cell culture was continued by adding fresh serum-free medium. The migration of cells at the edge of the scratch was observed and photographed using an inverted phase-contrast microscope at different times (0 h and 48 h). The relative distance that the healing scratch traveled was measured to calculate the healing rate. Wound healing rate (%) = (Scratch distance at 0 h-scratch distance at 48 h)/scratch distance at 0 h ×100%.

Transwell cell migration assay

A layer of Matrigel (diluted to 1:5 with serum-free culture medium, 50 μL/well, incubated for 30 min at 37°C for gel formation) was applied on the Corning chamber filter. Four hundred microliters of serum-free medium containing 3×10^4 cells were seeded into the upper chamber, and 600 μL of culture medium containing 10% serum was added to the lower chamber. After 24 h of routine incubation, the Matrigel and cells in the upper chamber were wiped off, fixed in paraformaldehyde, stained with crystal violet for 5 min, and photographed under a microscope at 200× magnification. Five microscopic fields were randomly selected for cell counting and the mean values were obtained.

Tumor metastasis assay in mice

Forty NOD/SCID mice (male:female is 1:1) aged 4-5 weeks old were purchased from Shanghai Laboratory Animal Center, China and kept under specific pathogen-free (SPF) conditions for 1 week for acclimatization. Approximately 1×10^6 cells were suspended in 150 μL of PBS and were injected into the mice via the tail vein. The mice were divided into four groups according to the injected cell suspension type, namely the MEG3, Vector NC, shRNA MEG3, and shRNA NC groups, with 10 mice in each group. After the mice died, the survival curves were calculated and the tumor foci on the lung surface were observed visually and counted. The lung tissues were then fixed with 10% paraformaldehyde, dehydrated, cleared, waxed, embedded as per routine practices, prepared into 3 μm paraffin sections, stained, and observed under a light microscope according to the conventional protocol. The experimental procedure was approved by the Ethics Committee of the Shenzhen People's Hospital.

In vivo fluorescence imaging of mice

Fluorescence imaging of mice was performed on day 10 and day 20 after Luc-GFP-labeled cells were intravenously injected into nude mice via tail. The *in vivo* molecular imaging system was switched on and pre-cooled for 20 min. The mice were weighed and intraperitoneally injected with 200 mg/kg of the fluorescent substrate. Ten minutes after injection, the mice were placed in the *in vivo* imager and each

mouse was observed for 2 min. The mice remained anesthetized with isoflurane throughout the operation. *In vivo* imaging results were analyzed with Lumina II living image 4.3 software. The analysis area of a 3.2 cm diameter circle in the lung was selected for each mouse, and the total fluorescence intensity and the average fluorescence intensity of each mouse were calculated. A log 10 conversion was conducted for the fluorescence intensity values.

Electrophoretic mobility shift assay (EMSA)

RNA EMSA was performed using the LightShift Chemiluminescent EMSA Kit (Pierce, USA). After harvest, a cytoplasmic protein lysis buffer was added to the cells and the cells were lysed on ice for 40 min, centrifuged at 4°C and 14,000×g for 5 min. The supernatant was cytoplasmic protein, which was discarded, and the nuclear protein lysate was added to lyse the resuspended precipitate on ice for 1 h. After centrifugation at 4°C for 20 min (14,000×g), the supernatant obtained was the nuclear protein extract. The biotin-labeled MEG3 probe or unlabeled complementary RNA probe was incubated with the nuclear protein extract (5 μg protein) for 30 min at room temperature. Electrophoresis was carried out using a 6% non-denaturing polyacrylamide gel (100 V, 55 min), which was then transferred to a nylon membrane at 380 mA for 40 min. The nylon membrane was blocked with a blocking solution for 15 min and incubated with streptavidin horseradish peroxidase antibody for 30 min before incubating with the equilibration solution for 15 min. Finally, a chemiluminescent solution was added for imaging with the chemiluminescent gel imaging system. For supershift analysis, 200 ng of anti-β-catenin, anti-GSK-3β antibody (Cell Signaling Technology, MA, USA), or IgG was added to the binding reactions of protein-lnc RNA before fluorescence gel imaging.

RNA pull down

RNA pull-down assays were performed using the Pierce Streptavidin Magnetic Beads Kit (Thermo Scientific, USA). Cells were lysed with the lysis buffer containing 1% RNase inhibitor and 1% protease inhibitor cocktail for western blotting and immunoprecipitation (IP) to extract the cellular proteins. Five picomoles of biotin-labeled MEG3 was added *in vitro* to the structured buffer to allow the formation of the secondary structure of RNA. Folded RNA was incubated with 2 mg of protein lysis buffer at room temperature for 1 h. After washing with the IP buffer three times, the incubated protein-RNA complex was added to an EP tube containing magnetic beads and incubated for 1 h at room temperature on a shaker. The beads were removed by centrifugation after washing with the IP buffer three times. The samples were subjected to SDS-PAGE electrophoresis, mass spectrometry, and validation by western blotting.

RNA immunoprecipitation (RIP)

The RIP assay was performed using the EZ-Magna RIP™ RNA-Binding Protein Immunoprecipitation Kit (Sigma, USA). Cells in the logarithmic phase were lysed by adding the RIP lysis buffer. Fifty microliters of magnetic beads were incubated with 5 μg of antibody at room temperature with rotation for 30 min to allow the binding of the antibody to the magnetic beads. One hundred and fifty microliters of the cell lysate supernatant and 900 μL of RIP buffer were added to the bead-antibody complex, which was incubated for 8 h at 4°C. The incubated reaction solution was placed on a magnetic stand, and the supernatant was discarded. To each tube, 500 μL of RIP wash buffer was added, and this was repeated six times. Proteinase K buffer (150 μL) was added to incubate for 30 min at 55°C. After digestion, the EP tubes were placed on a magnetic stand, the supernatant was transferred to new tubes, and 250 μL of RIP wash buffer was added to each tube. RNA was purified and recovered using an RNeasy Mini Kit, and qRT-PCR was performed after reverse transcription.

Co-immunoprecipitation (CO-IP)

CO-IP experiments were conducted using the Pierce Classic Magnetic IP/Co-IP Kit (Thermo Scientific, USA). Cells were collected, and 300 μL of cell lysis buffer was added. After sonicating at 100 W for 5 seconds, the tubes were rotated vertically at 4°C for 30 min. Three μg of anti-β-catenin antibody (or anti-GSK-3β antibody) was added to the supernatant and incubated at 4°C overnight with vertical rotation. After the incubation, the protein lysate was transferred to an EP tube containing protein A/G-magnetic beads and incubated for 2 h at 4°C on a rotating wheel. Next, the EP tube was

removed, placed on a magnetic stand, and the supernatant was removed. The remaining portions were the bead-antigen-antibody complex. After washing with PBST and the dilute buffer, the complex was placed in boiling water for 8-10 min, then placed on a magnetic stand. The supernatant was transferred into a new EP tube to obtain the desired antigen-antibody complex and cooled on ice for SDS-PAGE electrophoresis. Then, the membrane was transferred, blocked for 1 h, incubated with the primary antibody on a shaker at 4°C overnight. Finally, the membrane was washed, incubated with the secondary antibody at room temperature for 1 h, and developed.

Ubiquitination assay

Forty-eight hours after transfection with plasmid HA-Ubiquitin, the cells were pretreated with proteasome inhibitor MG132 at a concentration of 20 μmol/L for 4 h. The cells were then lysed by adding 500 μL of M2 buffer containing N-ethylmaleimide (NEM, concentration 0.8 mmol/L) and ubiquitin acetaldehyde (concentration 5 μmol/L). Protein A/G conjugated with β-catenin antibody was added to the lysate, and the cells were immunoprecipitated overnight at 4°C, and a western blotting was performed with ubiquitin as the antibody to detect the extent of ubiquitination of the target protein.

Cycloheximide (CHX)-chase assay

The CHX-chase assay was performed using the inhibitor of protein synthesis CHX (Selleck-Chemicals). CHX (12.5 μg/mL) was added to each group of cells for cell culture, and Western blotting analysis was performed at 0, 3, 6, 12, and 24 h to measure the expression of target proteins.

Statistical analyses

Statistical analyses were performed using the SPSS software package (version 20.0, SPSS Inc.). All tests were repeated three times and expressed as the mean ± SD. The t-test was used for the comparison between two independent samples. The analysis of variance was used for the comparison of data between multiple groups and the LSD-t test was used for the comparison between groups. A $P \leq 0.05$ was considered a statistically significant difference.

Results

Validation of MEG3 expression in retinoblastoma tissue using the GEO database

Our previous study confirmed the low expression of MEG3 in retinoblastoma tissues [11]. In this study, further validation and analysis were made using the GEO database. First, we analyzed three retinoblastoma tissues and the corresponding normal retina samples using the GSE110811 database and found that the expression of 114 genes was significantly decreased, whereas the expression of 22 genes was significantly increased in retinoblastoma tissues. Further analysis revealed that MEG3 was the one of the most differentially expressed gene and was significantly decreased in retinoblastoma tissues (Log2 FC=-3.1, $P<0.05$, **Figure 1A**, **1B**). Next, we compared GSE5222 (12 retinoblastoma tissues) and GSE28133 (19 normal retina samples) and found that MEG3 was significantly under-expressed in retinoblastoma tissues ($P<0.05$, **Figure 1C**, **1D**). Finally, we analyzed our previous study data and found that the expression of MEG3 was not only low in retinoblastoma tissues but was lower in metastatic retinoblastoma tissues than in non-metastatic retinoblastoma tissues, and the difference was statistically significant ($P<0.05$, **Figure 1E**).

Determining the effect of MEG3 on the invasion and migration of retinoblastoma cells in vitro

We found that MEG3 expression was lowest in Weri-Rb1 cells, followed by Y79 cells and highest in human retinal pigment epithelium hTERT RPE-1 cells ($P<0.05$, Figure S1A). So, we constructed a Weri-Rb1 cell line with stable high expression of MEG3 and a Y79 cell line with stable low expression of MEG3 using lentiviral vectors. The qRT-PCR results showed that the Weri-Rb1 cells in the MEG3 group (MEG3) had significantly increased expression of Weri-Rb1 compared with the blank control group (vector NC) ($P<0.05$, Figure S1B), whereas compared with the control group (shRNA NC), Y79 cells in the shRNA MEG3 group (shRNA MEG3) had significantly reduced MEG3 expression ($P<0.05$, Figure S1B).

Transwell assay results showed that the Weri-Rb1 cells in the MEG3 group had a significantly

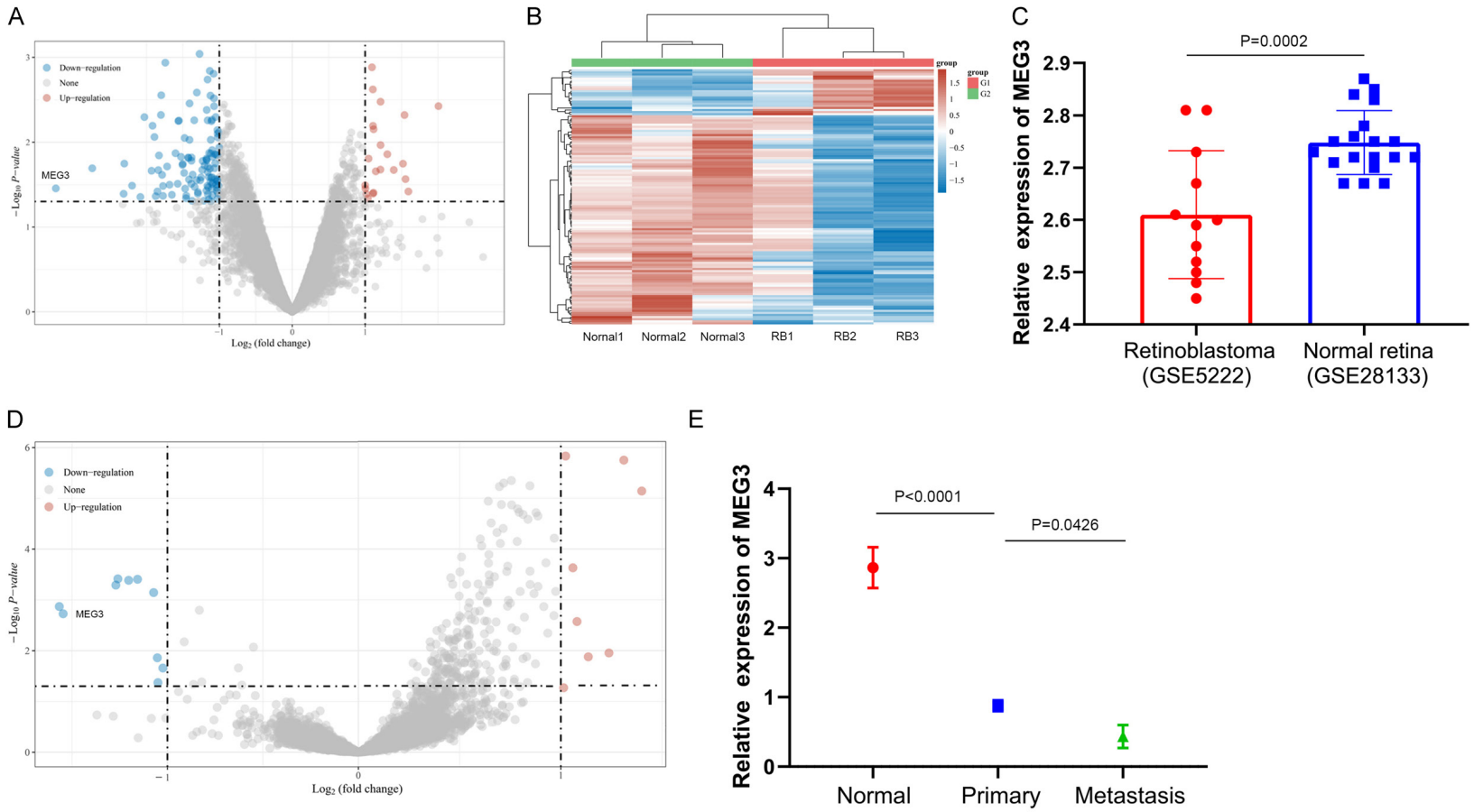

Figure 1. Low expression of MEG3 in retinoblastoma tissues. A, B. GSE110811 RNA-Seq database analysis showed low expression of MEG3 in retinoblastoma tissues (three retinoblastoma tissues vs. three paired normal retina samples). C, D. GSE5222 (12 retinoblastoma tissues) and GSE28133 (19 normal retina samples) RNA-Seq databases showed low expression of MEG3 in retinoblastoma tissues. E. MEG3 expression was lower in metastatic retinoblastoma tissues than in non-metastatic tissues.

lower number of invasive cells that had crossed the Matrigel compared to the blank controls (P<0.05, **Figure 2A**), whereas Y79 cells in the shRNA MEG3 group had a significantly higher number of invasive cells that had crossed the Matrigel compared to the controls (P<0.05, **Figure 2A**). The above results suggested that MEG3 could inhibit the invasion of retinoblastoma cells. The scratch test showed that the wound healing rate of Weri-Rb1 cells in the MEG3 group at 48 h was significantly lower than that of the blank control group (P<0.05, **Figure 2B**), whereas the wound healing rate of Y79 cells in the shRNA MEG3 group at 48 h was significantly higher than that of the control group (P<0.05, **Figure 2B**). These results indicated that MEG3 could inhibit the migration of retinoblastoma cells.

Determining the effect of MEG3 on the metastasis of retinoblastoma in vivo

Forty mice were divided equally into four groups and were injected with MEG3, Vector NC, shRNA MEG3, or shRNA NC cells via the tail vein. We sacrificed the mice by CO_2 inhalation when they have cachexia (including not eating, not moving, etc.), and autopsies revealed a variable number of white, round-like tumor foci on the lung surface in all mice. The number of tumors in the MEG3 and shRNA MEG3 group was significantly lower compared with the control group (P<0.05, **Figure 2C**). When the lung tissues were observed under a light microscope, only a small number of infiltrating cancer cells were visible in the MEG3 group, and much of the normal lung tissue was observed, whereas in the shRNA MEG3 group, more closely arranged, round- or oval-shaped cancer cells with large deeply stained nuclei were seen, and the normal lung tissues were severely damaged. Furthermore, the qRT-PCR results of metastatic tumor foci showed that the expression of MEG3 in the metastatic foci in the MEG3 group was significantly higher than that of the control tissues. In contrast, the expression of MEG3 in the metastatic foci of the shRNA MEG3 group was significantly lower than that of the control tissues (P<0.05, **Figure 2C**). Survival curve analysis showed that the survival time of mice in the MEG3 group was significantly longer than that in the vector NC group, whereas the survival time of mice in the shRNA MEG3 group was significantly shorter than that in the shRNA NC group (P<0.05, **Figure 2C**).

Additionally, nude mice were injected with luciferase-labeled retinoblastoma cell line via the tail vein, and the mouse live imaging system detected the expression of luciferin after 10 d and 20 d. The results showed that the fluorescent signal observed in the lungs of the nude mice in the MEG3 group was significantly lower than that of the vector NC group, and the growth rate of the fluorescent signal in the lungs of the nude mice in the MEG3 group was significantly lower than that of the vector NC group. However, the fluorescent signals observed in the lungs of the nude mice in the shRNA MEG3 group were significantly stronger than those of the shRNA NC group, and the growth rate of fluorescent signals in the lungs of the nude mice in the shRNA MEG3 group was significantly higher than that of vector NC (P<0.05, **Figure 2D**).

MEG3 binds to β-catenin and GSK-3β

We performed the Kyoto Encyclopedia of Genes and Genomes (KEGG) and gene ontology (GO) pathway enrichment analysis using the GSE110811 database. KEGG analysis suggested that the significantly down-regulated genes in retinoblastoma tissues were mainly enriched in Wnt signaling pathway and invasion of cells. GO analysis suggested that genes significantly down-regulated in retinoblastoma tissues were mainly enriched in focal adhesion, adherens junction, cell-substrate adherens junction, and anchoring junction (AJP) (**Figure 3A**). Additionally, gene interaction analysis indicated that MEG3 was associated with the the Wnt pathway (**Figure 3B**).

We then performed the RNA pull-down assay to identify the proteins that bind to MEG3. After isolating and purifying the proteins bound to the MEG3 probe, protein mass spectrometry and western blotting analysis were performed. It was found that MEG3 could bind to β-catenin, a core protein of the Wnt pathway, as well as GSK-3β (**Figure 3C**). Furthermore, EMSA results showed that the biotin-labeled MEG3 probe could bind to nucleoproteins, showing a shifted band, whereas the shifted band disappeared after adding non-labeled competing probes. After the addition of anti-β-catenin or GSK-3β antibodies, supershifted bands appe-

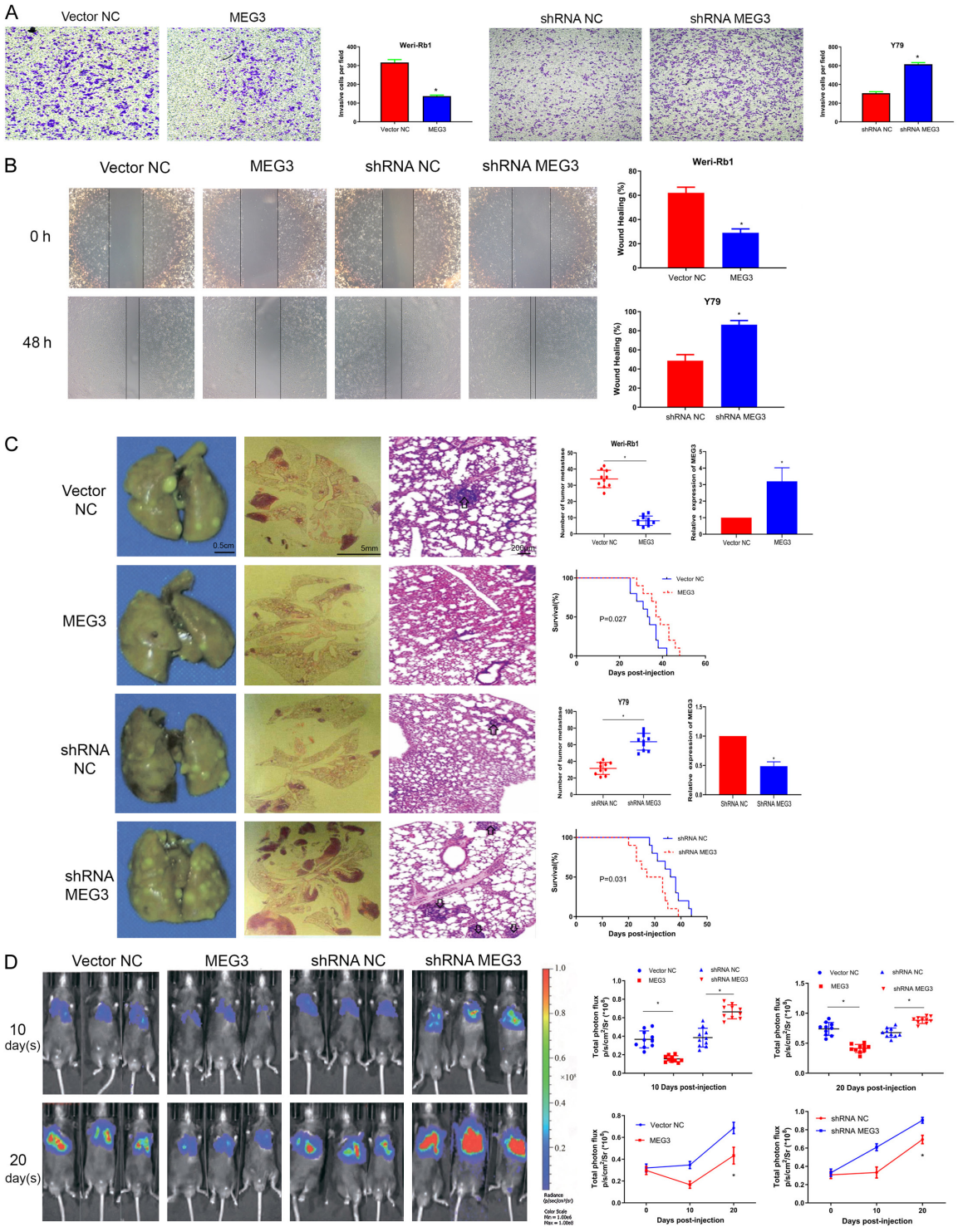

Figure 2. MEG3 inhibits the invasion and migration of retinoblastoma cells. A. Transwell assay showed that upregulation of MEG3 inhibited Weri-Rb1 cell invasion and downregulation of MEG3 promoted Y79 cell invasion. B. Scratch assay showed that upregulation of MEG3 inhibited Weri-Rb1 cell migration and downregulation of MEG3 promoted Y79 cell migration. C. Comparison of the number of lung tumor lesions, pathological tests, and survival rates of mice after injection of retinoblastoma cells via the tail vein. D. Nude mice were injected with a luciferase-labeled retinoblastoma cell line via tail vein, and the expression of luciferin was detected in vitro by a live imaging system. *P<0.05.

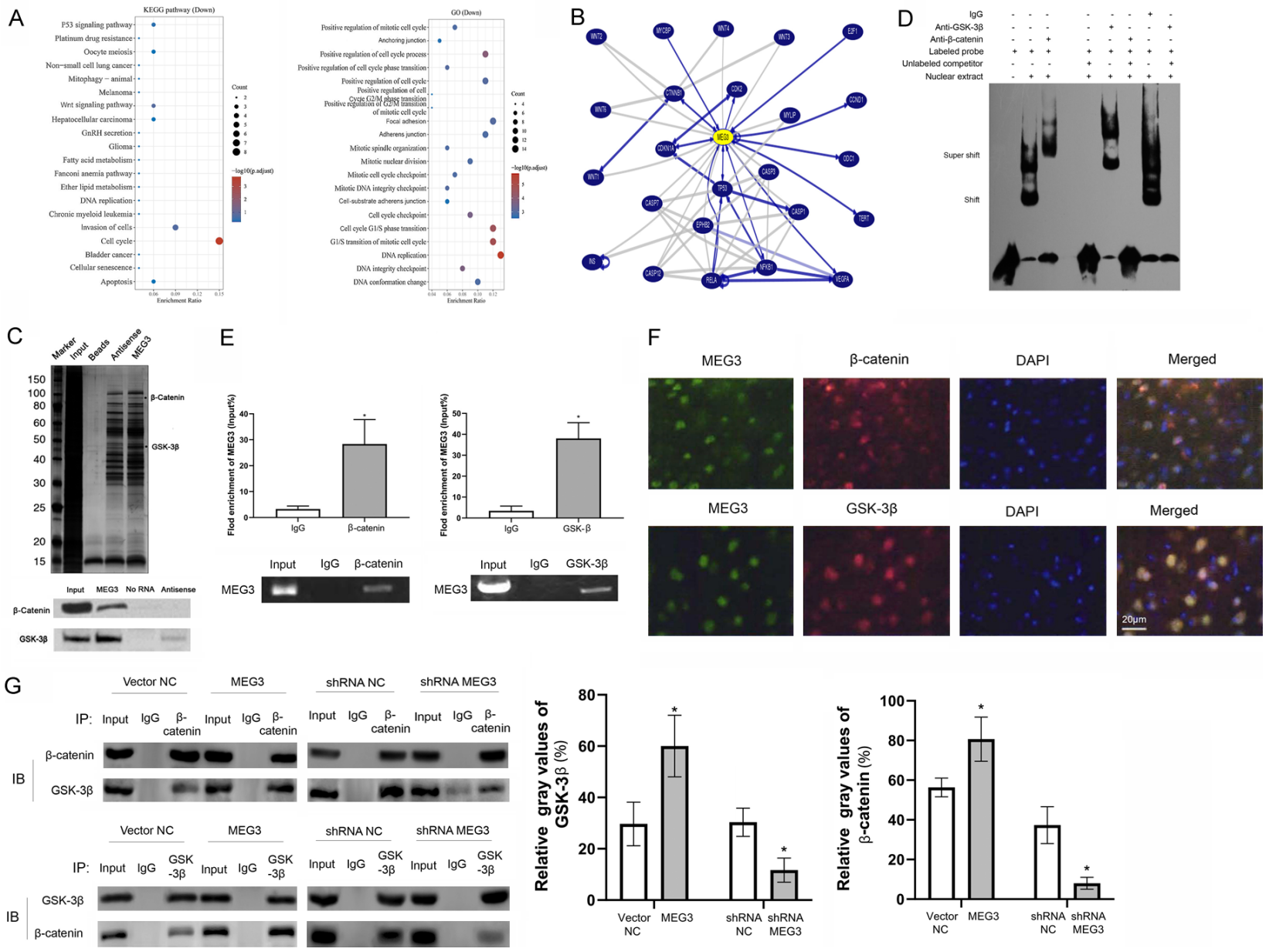
A
KEGG pathway (Down)
P53 signaling pathway
Platinum drug resistance
Oocyte meiosis
Non−small cell lung cancer
Mitophagy − animal
Melanoma
Wnt signaling pathway
Hepatocellular carcinoma
GnRH secretion
Glioma
Fatty acid metabolism
Fanconi anemia pathway
Ether lipid metabolism
DNA replication
Chronic myeloid leukemia
Invasion of cells
Cell cycle
Bladder cancer
Cellular senescence
Apoptosis
Enrichment Ratio
GO (Down)
Positive regulation of mitotic cell cycle
Anchoring junction
Positive regulation of cell cycle process
Positive regulation of cell cycle phase transition
Positive regulation of cell cycle
Positive regulation of cell cycle G2/M phase transition
Positive regulation of G2/M transition of mitotic cell cycle
Focal adhesion
Adherens junction
Mitotic spindle organization
Mitotic nuclear division
Mitotic cell cycle checkpoint
Mitotic DNA integrity checkpoint
Cell-substrate adherens junction
Cell cycle checkpoint
Cell cycle G1/S phase transition
G1/S transition of mitotic cell cycle
DNA replication
DNA integrity checkpoint
DNA conformation change
Enrichment Ratio
B
WNT2
MYO5B
WNT4
WNT3
EIF1
CTNNB1
CDK2
WNT8
CCND1
MYLP
MEG3
CDKN1A
CDC1
WNT1
CASP3
TP53
CASP7
CASP1
TERT
EPHB2
IKS
CASP12
RELA
NFKB1
VEGFA
C
Marker
Input
Beads
Antisense
MEG3
150
100
80
60
50
40
30
25
20
15
β-Catenin
GSK-3β
Input
MEG3
No RNA
Antisense
β-Catenin
GSK-3β
D
IgG
Anti-GSK-3β
Anti-β-catenin
Labeled probe
Unlabeled competitor
Nuclear extract
Super shift
Shift
E
Flod enrichment of MEG3 (Input%)
IgG
β-catenin
Flod enrichment of MEG3 (Input%)
IgG
GSK-β
Input
IgG
β-catenin
MEG3
Input
IgG
GSK-3β
MEG3
F
MEG3
β-catenin
DAPI
Merged
MEG3
GSK-3β
DAPI
Merged
20μm
G
Vector NC
MEG3
shRNA NC
shRNA MEG3
IP:
Input
IgG
β-catenin
IB
β-catenin
GSK-3β
Vector NC
MEG3
shRNA NC
shRNA MEG3
IP:
Input
IgG
GSK-3β
IB
GSK-3β
β-catenin
Relative gray values of GSK-3β (%)
Vector NC
MEG3
shRNA NC
shRNA MEG3
Relative gray values of β-catenin (%)
Vector NC
MEG3
shRNA NC
shRNA MEG3

Figure 3. MEG3 binds to β-catenin and GSK-3β. A. KEGG and GO analysis of the enrichment of abnormally down-regulated genes in retinoblastoma tissues in the pathway. B. GSE110811 RNA-Seq database analysis of MEG3-associated genes. C. RNA pull-down assay to analyze the binding proteins of MEG3. D. EMSA to analyze the binding proteins of MEG3. E. RIP assay to analyze the binding RNA of β-catenin and GSK-3β. F. Co-localization of MEG3 and β-catenin/MEG3 and GSK-3β by double immunofluorescence. G. CO-IP assay to analyze the effect of MEG3 on the binding of β-catenin and GSK-3β. *P<0.05.

ared in all lanes, which indicated possible binding of MEG3 to β-catenin and GSK-3β (**Figure 3D**). Next, we used the RIP assay to identify lncRNAs that could bind to β-catenin or GSK-3β. After isolating and purifying RNAs that bound to β-catenin or GSK-3β, RT-qPCR and gel electrophoresis were performed, and it was found that β-catenin and GSK-3β could bind with MEG3 (P<0.05, **Figure 3E**). The results of double-labeled immunofluorescence staining also showed that MEG3 (red fluorescence), β-catenin (green fluorescence) and GSK-3β (green fluorescence) were expressed in Rb cells. After the images were merged, the green and red fluorescence overlapped, indicating that MEG3 co-localized with β-catenin (green fluorescence) and GSK-3β (green fluorescence) in Rb cells (**Figure 3F**). Finally, we performed Co-IP assays to analyze whether MEG3 could promote the binding of β-catenin to GSK-3β. We first used the β-catenin antibody as the decoy protein, and the results showed that the MEG3 group bound to more GSK-3β proteins during Co-IP than the control group, whereas the shRNA MEG3 group could bind to less GSK-3β protein during Co-IP compared with the control group (P<0.05, **Figure 3G**). Next, the GSK-3β antibody was used as the decoy protein, and the results again showed that the MEG3 group exhibited increased binding to β-catenin during Co-IP compared with the control group, whereas the shRNA MEG3 group exhibited decreased binding to β-catenin during Co-IP compared with the control group (P<0.05, **Figure 3G**).

MEG3 promotes β-catenin degradation through the ubiquitin-proteasome system

We first examined the distribution of MEG3 in retinoblastoma cells, and the results showed that MEG3 was distributed in both cytoplasm and nucleus (Figure S1C). Next, we examined the transcription levels of β-catenin and GSK-3β genes, and the RT-qPCR results showed that the transcription levels of β-catenin and GSK-3β genes were not significantly changed after MEG3 were up- or down-regulated (P>0.05, Figure S1D, S1E). Furthermore, we examined the protein expression levels of β-catenin and GSK-3β, and the western blotting results showed that the expression levels of GSK-3β were not significantly changed after MEG3 were up- or down-regulated (Figure S1F). However, the expression of β-catenin protein was lower in the MEG3 group than in the control group, whereas the expression of β-catenin protein in the shRNA MEG3 group was higher than that of the control group. But the phosphorylation level of β-catenin was significantly higher in the MEG3 group than in the control group, whereas the phosphorylation level of β-catenin in the shRNA MEG3 group was significantly lower than that of the control group, suggesting that MEG3 could regulate the phosphorylation level of β-catenin (Figure S1F). We then verified the protein expression levels of β-catenin in 63 retinoblastoma tissues. The western blotting results showed that the expression of β-catenin in Metastasis retinoblastoma tissues was significantly higher than in Primary retinoblastoma tissues and in the paired paracancerous normal retinal tissues (P<0.05, **Figure 4A**). Furthermore, Pearson correlation analysis was performed, and MEG3 was negatively correlated with β-catenin in Metastasis retinoblastoma tissues, Primary retinoblastoma tissues and the paired paracancerous normal retinal tissues. The correlation coefficient between the MEG3 and β-catenin showed an increasing trend in paired paracancerous normal retinal tissues, Primary retinoblastoma tissues and Metastasis retinoblastoma tissues (**Figure 4B**).

Next, retinoblastoma cells were treated with the protein synthesis inhibitor CHX for 0 h, 3 h, 6 h, 12 h, and 24 h, and a western blotting was performed to detect the changes in protein expression levels of β-catenin in retinoblastoma cells after the addition of the inhibitor. The results indicated that the protein degradation in cells in the MEG3 group was significantly faster than the control cells, whereas the degradation of β-catenin protein in cells in the shRNA-MEG3 group was significantly slower than

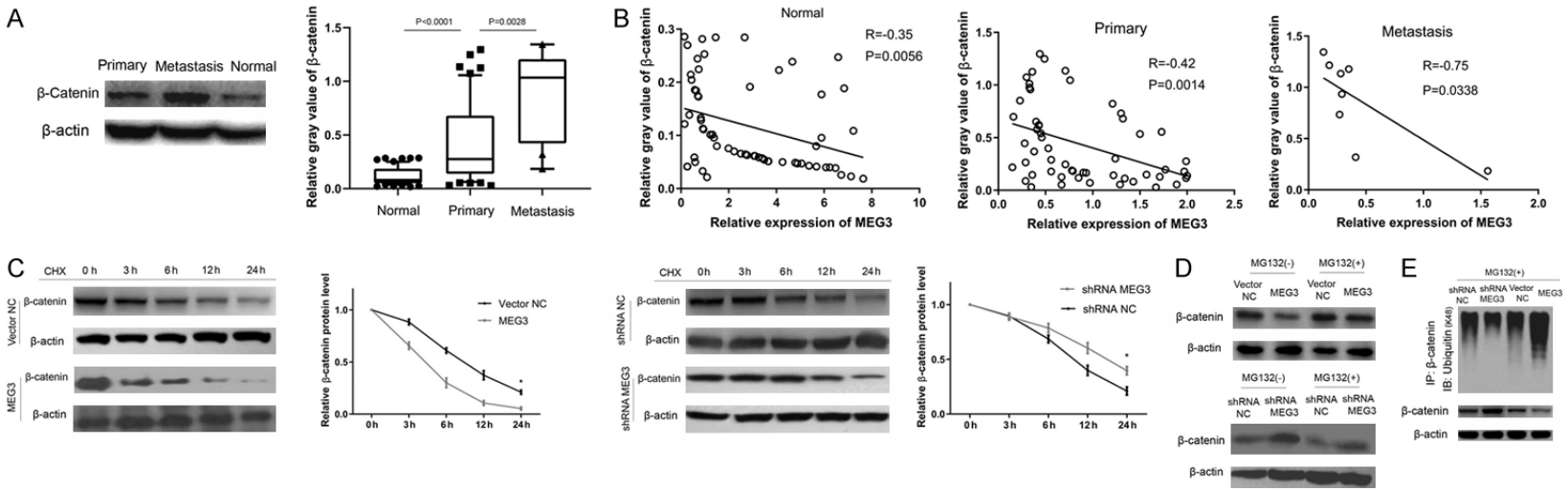

Figure 4. MEG3 promotes the degradation of β-catenin by the ubiquitin-proteasome system. A. Comparing the expression levels of β-catenin in Normal retina tissues, Primary retinoblastoma tissues and Metastasis retinoblastoma tissues using the western blotting assay. B. Pearson correlation analysis of the correlation between the expression levels of MEG3 and β-catenin in Normal retina tissues, Primary retinoblastoma tissues and Metastasis retinoblastoma tissues. C. CHX assay suggested that MEG3 promoted the degradation of β-catenin. D. MG132 assay suggested that MEG3 promoted ubiquitin-dependent proteasomal degradation of β-catenin. E. Ubiquitination assays suggested that MEG3 promoted the ubiquitination of β-catenin. *P<0.05.

the control cells (P<0.05, **Figure 4C**). Additionally, retinoblastoma cells were also treated with the proteasome inhibitor MG132 and the changes in β-catenin protein expression levels in the cells were determined by western blotting. The results showed that compared with the MG132 (-) control group, the β-catenin protein expression levels in cells with high MEG3 expression in the MG132 (+) treatment group were higher than that in the control group (vector NC), whereas the β-catenin protein expression levels in cells with low MEG3 expression were lower than that in the control group (shRNA NC) (**Figure 4D**). Finally, the results of ubiquitination assays suggested that β-catenin protein exhibited higher ubiquitination levels in retinoblastoma cells with high MEG3 expression than the controls. In contrast, in retinoblastoma cells with low MEG3 expression, β-catenin protein had lower ubiquitination levels than the controls (**Figure 4E**).

MEG3 degrades β-catenin protein through ubiquitination via GSK-3β

The western blotting results showed that the Phosphorylation ratio of GSK-3β in Metastasis retinoblastoma tissues was significantly lower than in Primary retinoblastoma tissues and in the paired paracancerous normal retinal tissues (P<0.05, Figure S1G). Then the western blotting results confirmed the high expression of β-catenin in Rb cells after transfection of with shRNA-GSK-3β (**Figure 5A**). Furthermore, the results of ubiquitination assays suggested that β-catenin protein exhibited higher ubiquitination levels in retinoblastoma cells with high GSK-3β expression than the controls. In contrast, in retinoblastoma cells with low GSK-3β expression, β-catenin protein had lower ubiquitination levels than the controls (Figure S1H).

Then Weri-Rb1 cells were transiently transfected with pcDNA MEG3 and pcDNA NC, and RT-qPCR showed that compared with controls. Transfection with pcDNA NC and Weri-Rb1 cells with pcDNA MEG3 showed overexpression of MEG3, and the difference was statistically significant (Figure S1I, P<0.05). We examined the change in the regulation of MEG3 on the expression and function of β-catenin in Weri-Rb1 cells under low expression levels of GSK-3β. First, western blotting showed no significant change in β-catenin expression levels in the shRNA-GSK-3β + pcDNA NC group compared with the shRNA-GSK-3β + pcDNA MEG3 group. The β-catenin expression level was also not significantly changed in the shRNA-GSK-3β + si NC group compared with the shRNA-GSK-3β + si MEG3 group (**Figure 5B**), suggesting that the regulation of MEG3 on β-catenin expression was significantly diminished under low expression of GSK-3β. After using GSK-3β overexpression vector to rescue (shGSK-3β + MEG3) cells, we found that MEG3 could reduce the β-catenin expression again in Rb cells which strongly proved that MEG3 regulated β-catenin via GSK-3β (**Figure 5C**). Second, the results of ubiquitination assays suggested that there was no significant difference in ubiquitination of β-catenin in the shRNA-GSK-3β + pcDNA NC group compared with the shRNA-GSK-3β + pcDNA MEG3 group. In contrast, the ubiquitination level of β-catenin was also not significantly different in the shRNA-GSK-3β + si NC group compared with the shRNA-GSK-3β + si MEG3 group (**Figure 5D**), suggesting that the ubiquitination of β-catenin by MEG3 was significantly weakened under low expression of GSK-3β. Finally, the results of the Transwell assays suggested that there was no significant difference in the number of invading cells that had crossed the Matrigel in the shRNA-GSK-3β + pcDNA NC group compared with the shRNA-GSK-3β + pcDNA MEG3 group. The number of invading cells that had crossed the Matrigel was also not significantly different in the shRNA-GSK-3β + si NC group compared with the shRNA-GSK-3β + si MEG3 group (P<0.05, **Figure 5E**), suggesting that the regulatory effect of MEG3 on the invasion of retinoblastoma cells was significantly diminished under low expression of GSK-3β.

Discussion

Previous studies have confirmed that LncRNAs play an important role in the occurrence and invasion of retinoblastoma [13, 14]. We analyzed the MEG3 expression in 63 retinoblastoma tissues in a previous study and found that the MEG3 gene was inactivated in retinoblastoma tissues [11, 12]. Combined with the fact that MEG3 has been shown to have low expression in various tumors and is an important tumor suppressor gene [6-8], we hypothesized that MEG3 plays a similar tumor suppressor role in retinoblastomas. However, the strength of evidence was compromised because the

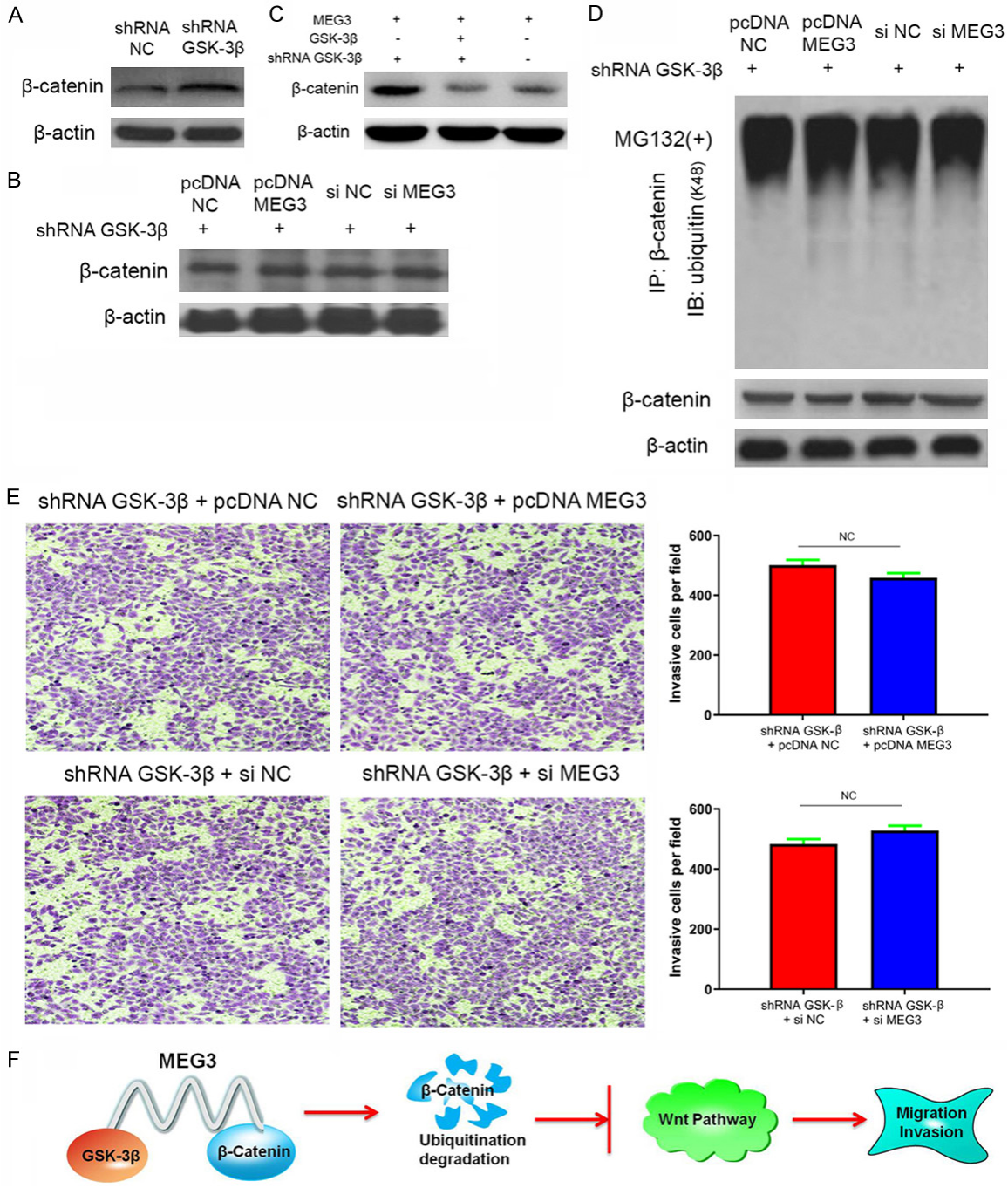

Figure 5. MEG3 promotes ubiquitination and degradation of β-catenin by GSK-3β. A. Western blotting assays suggested that β-catenin protein expression is increased in retinoblastoma cells stably transfected with shRNA-GSK-3β. B. Western blotting assays suggested that MEG3 had no significant regulatory effect on β-catenin expression in retinoblastoma cells with low GSK-3β protein expression. C. Rescue assays of GSK-3β overexpression in (shGSK-3β + MEG3) cells. D. Ubiquitination assays suggested that in retinoblastoma cells with low expression of GSK-3β, MEG3 had no significant effect on the ubiquitination of β-catenin. E. Transwell assays showed no obvious regulatory effects of MEG3 on the invasion of retinoblastoma cells in retinoblastoma cells with low GSK-3β expression. F. Schematic diagram of the regulatory pathway of MEG3 on β-catenin. *P<0.05.

conclusion was derived from our single-center specimen analysis results and lacked the validation of multicenter specimens. Therefore, in this study, we used the GEO database to ana-

lyze the MEG3 expression in retinoblastoma specimens from other hospitals to reduce statistical errors. Both the GSE110811 and GSE5222 databases suggested significant inactivation of MEG3 in retinoblastoma tissues, consistent with our previous findings, and with the low expression of MEG3 in other tumors, which again demonstrated the reliability of our conclusions.

Our previous study found that the inactivation of MEG3 was closely associated with invasion and metastasis in retinoblastoma patients [11]. However, whether MEG3 can affect the invasion and metastasis of retinoblastoma cells remained unclear. Therefore, in this study, we explored the effect of MEG3 on the invasion and metastasis of retinoblastoma cells both *in vitro* and *in vivo*. The results of *in vitro* experiments, such as the scratch assay and the Transwell assay, and *in vivo* experiments, such as the mouse tumor metastasis assay and mouse fluorescence imaging assay, all confirmed that the inactivation of MEG3 could lead to enhanced migration and invasion of retinoblastoma cells, which could also explain why patients with low MEG3 expression are more prone to retinoblastoma cell invasion and metastasis.

To further investigate the mechanism by which MEG3 regulates the invasion and metastasis of retinoblastoma cells, we performed KEGG and GO analysis of the GSE110811 database and found that genes significantly down-regulated in retinoblastoma tissues were mainly enriched in the Wnt signaling pathway and MEG3 was associated with the core protein of the Wnt pathway. Additionally, Other scholars' studies also confirmed that the abnormal activation of the Wnt pathway was associated with tumor metastasis in retinoblastomas and Wnt pathway activator (LiCl)/inhibitor (Dkk1) could regulated the invasion of retinoblastoma cell lines via Wnt signaling pathway, which was consistent with our previous studies [11, 15-18]. Therefore, we speculated that MEG3 might affect the invasion and metastasis of retinoblastoma cells via regulating the activity of the Wnt pathway.

To further determine the specific molecular mechanism by which MEG3 regulates the activity of the Wnt pathway, we first analyzed the binding proteins of MEG3 using the RNA pull-down assay and the EMSA and found that MEG3 could bind to β-catenin and GSK-3β, two core proteins of the Wnt pathway. Next, we used the RIP assays to reversely verify the RNA bound to β-catenin and GSK-3β and found that both β-catenin and GSK-3β proteins were able to bind to MEG3. The above experiments demonstrated the interaction of MEG3 with β-catenin and GSK-3β. Subsequently, we found that MEG3 had no significant effect on the GSK-3β gene at either the mRNA transcription or protein translation levels. Although MEG3 exhibited non-significant effects on the β-catenin gene at the mRNA transcription level, a significant negative regulatory effect on the β-catenin gene at the protein level was observed. Therefore, we hypothesized that MEG3 exerted post-transcriptional regulation of β-catenin.

It has been shown that in hepatocellular carcinoma cells, MEG3 can directly bind to P53 protein and thereby affect the function of P53 protein [19]. In human pluripotent stem cells, MEG3 can also regulate the function of the PRC2 protein complex by binding to the JARID2 protein [20]. In breast cancer cells, MEG3 can also form a complex with EZH2 and the target gene promoter to regulate the expression of target genes [21]. In cervical cancer, MEG3 can bind to STAT3 and induce degradation of STAT3 by the ubiquitin-proteasome system [22]. The above study demonstrated that regulating the target protein function by binding to the target protein is a common form of post-transcriptional regulation of MEG3. Additionally, studies in the colon and hepatocellular carcinoma cells have confirmed the existence of an RNA binding region on β-catenin, which can bind to lncRNA to regulate the protein function [23, 24]. According to the above, we speculated that MEG3 might regulate the function of β-Catenin by binding to β-catenin.

GSK-3β acts as a switch molecule in Axin/GSK-3β/APC complex and regulates the Wnt pathway by phosphorylating β-catenin in Thr41, Ser37, and Ser33 sites. The phosphorylated β-catenin is ubiquitinated by ubiquitin ligase β-TrCP and then degraded via the ubiquitin-proteasome system [25]. Recent studies have demonstrated that lncRNAs can regulate the function of GSK-3β by binding to them, thereby regulating the Wnt pathway. For example, in both

dental pulp cells and lung adenocarcinoma cells, it was shown that lncRNA could regulate the phosphorylation of GSK-3β protein by binding to GSK-3β protein, thereby regulating the function of GSK-3β [26, 27]. Hu et al. further demonstrated that in gastric cancer cells, LncRNA-linc00261 could bind to both GSK-3β and the slug protein and enhance the degradation of the slug protein by GSK-3β protein through "molecular scaffolding", thus inhibiting the invasion and metastasis of gastric cancer cells [28]. In summary, the regulation of the invasion and metastasis of tumor cells by lncRNA through the regulation of the function of the GSK-3β protein by binding to it is a common form of action of lncRNA to perform its biological function.

Based on our finding that MEG3 binds to both GSK-3β and β-catenin, we speculated that MEG3 might indirectly promotes the ubiquitination and degradation of β-catenin through enhancing the phosphorylation of β-catenin by Axin/GSK-3β/APC complex. To confirm this, we first determined that MEG3 increased the binding of GSK-3β to β-catenin using the CO-IP assay, which revealed that promoting the binding of GSK-3β to β-catenin is an important molecular role of MEG3. Western Blot also indicated that MEG3 promoted the phosphorylation level of β-catenin. Based on the fact that Axin/GSK-3β/APC complex, rather than GSK-3β alone, phosphorylated β-catenin, we speculated that MEG3 enhanced the phosphorylation of β-catenin via Axin/GSK-3β/APC complex by promoting the binding of β-catenin to GSK-3β. Next, we treated the cells with cycloheximide (CHX), a protein synthesis inhibitor, and found that MEG3 accelerated the degradation of β-catenin. Additionally, MG132, a ubiquitination inhibitor, inhibited the pro-degradation effect of MEG3 on β-catenin. The ubiquitination assays also confirmed that MEG3 could promote the ubiquitination of β-catenin. The above results suggested that MEG3 may anchor β-catenin to the Axin/GSK-3β/APC complex by enhancing the binding of β-catenin to GSK-3β, promote β-catenin phosphorylation and accelerate β-catenin degradation via the ubiquitin-proteasome system.

Finally, to confirm that GSK-3β protein is a key bridge molecule for regulating the expression level of β-catenin by MEG3, we used shRNA to construct retinoblastoma cell lines with low expression of GSK-3β. Subsequently, it was found that the role of MEG3 in promoting ubiquitination of β-catenin protein, in regulating the expression level of β-catenin, and in promoting the biological function of retinoblastoma cell invasion were all significantly reduced. The above results confirmed that the GSK-3β protein is an important intermediate molecule for MEG3 to perform its molecular functions.

In conclusion, this study elucidated the molecular mechanism by which MEG3 inhibits the invasion and metastasis of retinoblastoma cells by reducing Wnt pathway activity through facilitating the phosphorylation, ubiquitination and degradation of β-catenin by GSK-3β (**Figure 5F**), which provided a new direction for exploring therapeutic approaches for metastatic retinoblastoma.

Acknowledgements

The Project Supported by National Natural Science Foundation of China (Grant No. 81902751), National Natural Science Foundation of China (Grant No. 81971385) and Natural Science Foundation of Guangdong Province (Grant No. 2019A1515010412).

Disclosure of conflict of interest

None.

Address correspondence to: Jun Zhang, Department of Reproductive Medicine, Obstetrics and Gynecology, Shenzhen People's Hospital (The Second Clinical Medical College, Jinan University), Shenzhen 518020, Guangdong, China. Tel: +86-0755-2294-8400; Fax: +86-0755-2294-8400; E-mail: zhangj49@mail2.sysu.edu.cn

References

[1] Martínez-Sánchez M, Hernandez-Monge J, Rangel M and Olivares-Illana V. Retinoblastoma: from discovery to clinical management. FEBS J 2021; [Epub ahead of print].

[2] Kaewkhaw R and Rojanaporn D. Retinoblastoma: etiology, modeling, and treatment. Cancers (Basel) 2020; 12: 2304.

[3] Jain M, Rojanaporn D, Chawla B, Sundar G, Gopal L and Khetan V. Retinoblastoma in Asia. Eye (Lond) 2019; 33: 87-96.

[4] Berry JL, Kogachi K, Murphree AL, Jubran R and Kim JW. A review of recurrent retinoblas-

toma: children's hospital Los Angeles classification and treatment guidelines. Int Ophthalmol Clin 2019; 59: 65-75.
[5] Fabian ID, Onadim Z, Karaa E, Duncan C, Chowdhury T, Scheimberg I, Ohnuma SI, Reddy MA and Sagoo MS. The management of retinoblastoma. Oncogene 2018; 37: 1551-1560.
[6] Zhang J, Lin ZQ, Gao YL and Yao TT. Downregulation of long noncoding RNA MEG3 is associated with poor prognosis and promoter hypermethylation in cervical cancer. J Exp Clin Cancer Res 2017; 36: 5.
[7] Zhang J, Yao TT, Wang YX, Yu J, Liu YY and Lin ZQ. Long noncoding RNA MEG3 is downregulated in cervical cancer and affects cell proliferation and apoptosis by regulating miR-21. Cancer Biol Ther 2016; 17: 104-113.
[8] Zhang J, Yao TT, Lin ZQ and Gao YL. Aberrant methylation of MEG3 functions as a potential plasma-based biomarker for cervical cancer. Sci Rep 2017; 7: 6271.
[9] Bian ZH, Zhang JW, Li M, Feng YY, Wang X, Zhang J, Yao SR, Jin GY, Du J, Han WF, Yin YF, Huang SL, Fei BJ, Zou J and Huang ZH. LncRNA-FEZF1-AS1 promotes tumor proliferation and metastasis in colorectal cancer by regulating PKM2 signaling. Clin Cancer Res 2018; 24: 4808-4819.
[10] He WM, Liang BS, Wang CL, Li SW, Zhao Y, Huang Q, Liu ZX, Yao ZQ, Wu QJ, Liao WJ, Zhang SY, Liu YJ, Xiang Y, Liu J and Shi M. MSC-regulated lncRNA MACC1-AS1 promotes stemness and chemoresistance through fatty acid oxidation in gastric cancer. Oncogene 2019; 38: 4637-4654.
[11] Gao YL and Lu XH. Decreased expression of MEG3 contributes to retinoblastoma progression and affects retinoblastoma cell growth by regulating the activity of Wnt/beta-catenin pathway. Tumour Biol 2016; 37: 1461-1469.
[12] Gao YL, Huang P and Zhang J. Hypermethylation of MEG3 promoter correlates with inactivation of MEG3 and poor prognosis in patients with retinoblastoma. J Transl Med 2017; 15: 268.
[13] Gao YL, Luo XL and Zhang J. Sp1-mediated upregulation of lnc00152 promotes invasion and metastasis of retinoblastoma cells via the miR-30d/SOX9/ZEB2 pathway. Cell Oncol (Dordr) 2021; 44: 61-76.
[14] Gao YL, Luo XL and Zhang J. LincRNA-ROR is activated by H3K27 acetylation and induces EMT in retinoblastoma by acting as a sponge of miR-32 to activate the notch signaling pathway. Cancer Gene Ther 2021; 28: 42-54.
[15] Silva AK, Yi H, Hayes SH, Seigel GM and Hackam AS. Lithium chloride regulates the proliferation of stem-like cells in retinoblastoma cell lines: a potential role for the canonical Wnt signaling pathway. Mol Vis 2010; 16: 36-45.
[16] Zhou XP, Wang YP, Li Q, Ma DH, Nie AQ and Shen XL. LncRNA Linc-PINT inhibits miR-523-3p to hamper retinoblastoma progression by upregulating Dickkopf-1 (DKK1). Biochem Biophys Res Commun 2020; 530: 47-53.
[17] Fu CB, Wang SC, Jin L, Zhang MM and Li MM. CircTET1 inhibits retinoblastoma progression via targeting miR-492 and miR-494-3p through Wnt/beta-catenin signaling pathway. Curr Eye Res 2021; 46: 978-987.
[18] Lyv XM, Wu F, Zhang H, Lu J, Wang L and Ma YH. Long noncoding RNA ZFPM2-AS1 knockdown restrains the development of retinoblastoma by modulating the microRNA-515/HOXA1/Wnt/beta-catenin axis. Invest Ophthalmol Vis Sci 2020; 61: 41.
[19] Zhu JJ, Liu SS, Ye FQ, Shen Y, Tie Y, Zhu J, Wei LX, Jin YH, Fu HJ, Wu YG and Zheng XF. Long noncoding RNA MEG3 interacts with p53 protein and regulates partial p53 target genes in hepatoma cells. PLoS One 2015; 10: e0139790.
[20] Kaneko S, Bonasio R, Saldaña-Meyer R, Yoshida T, Son J, Nishino K, Umezawa A and Reinberg D. Interactions between JARID2 and noncoding RNAs regulate PRC2 recruitment to chromatin. Mol Cell 2014; 53: 290-300.
[21] Mondal T, Subhash S, Vaid R, Enroth S, Uday S, Reinius B, Mitra S, Mohammed A, James AR, Hoberg E, Moustakas A, Gyllensten U, Jones SJ, Gustafsson CM, Sims AH, Westerlund F, Gorab E and Kanduri C. MEG3 long noncoding RNA regulates the TGF-β pathway genes through formation of RNA-DNA triplex structures. Nat Commun 2015; 6: 7743.
[22] Zhang J and Gao YL. Long non-coding RNA MEG3 inhibits cervical cancer cell growth by promoting degradation of P-STAT3 protein via ubiquitination. Cancer Cell Int 2019; 19: 175.
[23] Kim I, Kwak H, Lee HK, Hyun S and Jeong S. β-Catenin recognizes a specific RNA motif in the cyclooxygenase-2 mRNA 3'-UTR and interacts with HuR in colon cancer cells. Nucleic Acids Res 2012; 40: 6863-6872.
[24] Zhu PP, Wang YY, Huang GL, Ye BQ, Liu BY, Wu JY, Du Y, He L and Fan ZS. lnc-β-Catm elicits EZH2-dependent β-catenin stabilization and sustains liver CSC self-renewal. Nat Struct Mol Biol 2016; 23: 631-639.
[25] Jacobs KM, Bhave SR, Ferraro DJ, Jaboin JJ, Hallahan DE and Thotala D. GSK-3β: a bifunctional role in cell death pathways. Int J Cell Biol 2012; 2012: 930710.
[26] Chen LL, Song Z, Huang SH, Wang RF, Qin W, Guo J and Lin ZM. lncRNA DANCR suppresses odontoblast-like differentiation of human den-

tal pulp cells by inhibiting wnt/β-catenin pathway. Cell Tissue Res 2016; 364: 309-318.
[27] Zhang HY, Wang Y, Lu JB and Zhao YY. Long non-coding RNA LINC00222 regulates GSK3β activity and promotes cell apoptosis in lung adenocarcinoma. Biomed Pharmacother 2018; 106: 755-762.
[28] Yu YC, Li LJ, Zheng ZQ, Chen SR, Chen ED and Hu YR. Long non-coding RNA linc00261 suppresses gastric cancer progression via promoting Slug degradation. J Cell Mol Med 2017; 21: 955-967.

Table S1. Oligonucleotide sequence

Name	Sequence
MEG3 shRNA	5'-GGTTGTTGTGAGAATTAAA-3' (forward)
	5'-TTTAATTCTCACAACAACC-3' (reverse)
NC shRNA	5'-UAAUCCGAACGUGUCACGUTT-3' (forward)
	5'-ACGUGACACGUUCGGAGAATT-3' (reverse)
si-MEG3	5'-CCCUCUUGCUUGUCUUACUTT-3'

Table S2. PCR primers

Gene Name	Forward Primer (5'-3')	Reverse Primer (5'-3')
MEG3	5'-CATCCGTCCACCTCCTTGTCTTC-3'	5'-GTCCTCTTCATCCTTTGCCATCC-3'
β-catenin	5'-AGGGCAATCCTGAGGAAGAAGA-3'	5'-TGCGTGAAGGACTGGGAAAA-3'
GSK-3β	5'-GACTAAGGTCTTCCGACCCC-3'	5'-GCTTGAATCCGAGCATGAGG-3'
β-Actin	5'-GCACTCTTCCAGCCTTCCTTCC-3'	5'-GAGCCGCCGATCCACACG-3'

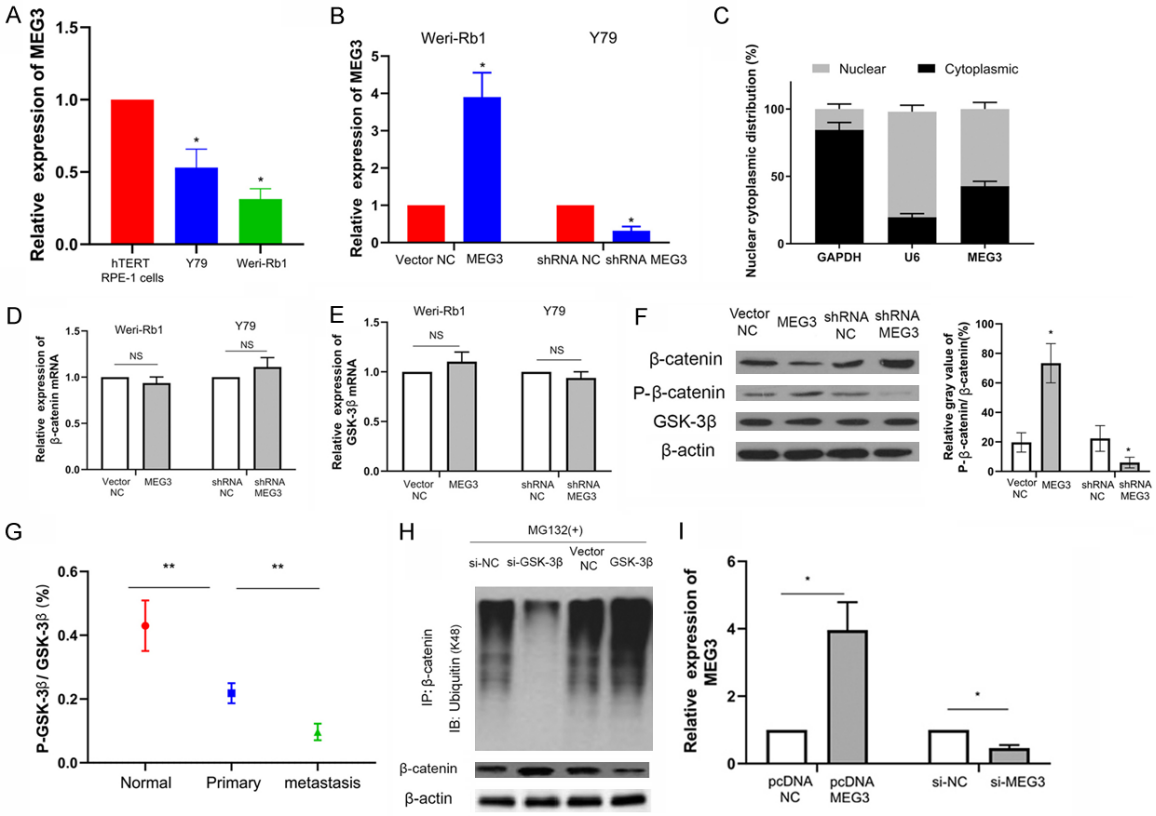

Figure S1. MEG3 inducted β-catenin degradation. A. Expression level of MEG3 in retinoblastoma Weri-Rb1 and Y79 cells and human retinal pigment epithelium hTERT RPE-1 cells. B. qRT-PCR analysis showed a significant increase in MEG3 expression in Weri-Rb1 cells stably transfected with MEG3 and a significant decrease in MEG3 expression in Y79 cells stably transfected with shRNA MEG3. C. Distribution of MEG3 in the cytoplasm and nucleus. D, E. RT-qPCR analysis of the effect of MEG3 on the transcription levels of β-catenin gene and GSK-3β gene. F. Determining the effect of MEG3 on the expression levels of phosphorylated β-catenin, β-catenin and GSK-3β using the western blotting assay. G. Comparing the phosphorylation levels of GSK-3β in Normal retina tissues, Primary retinoblastoma tissues and Metastasis retinoblastoma tissues using the western blotting assay. H. Ubiquitination assays suggested that GSK-3β promoted the ubiquitination of β-catenin. I. qRT-PCR results suggested a significant increase in MEG3 expression in retinoblastoma cells transfected with pcDNA-MEG3 and a significant decrease in MEG3 expression in retinoblastoma cells transfected with si-MEG3. *P<0.05, **P<0.01.